Zeitschrift: Helvetica Physica Acta

Band: 55 (1982)

Heft: 1

Artikel: Measurement of the average and longitudinal recoil polarizations in the reaction 12C(^-,)^12B(g.s.) : pseudoscalar coupling and neutrino helicity

Autor: Roesch, L.Ph. / Telegdi, V.L. / Truttmann, P.

DOI: https://doi.org/10.5169/seals-115280

Helvetica Physica Acta, Vol. 55 (1982) 74–99 0018–0238/82/010074–26$1.50 + 0.20/0

Measurement of the average and longitudinal recoil polarizations in the reaction $^{12}C(\mu^-, \nu)^{12}B$(g.s.): pseudoscalar coupling and neutrino helicity

L. Ph. Roesch, V. L. Telegdi, P. Truttmann and A. Zehnder,
Swiss Federal Institute of Technology, Laboratory for Nuclear Physics, CH-8093 Zürich, Switzerland,
L. Grenacs and L. Palffy, Institut de Physique Corpusculaire,
Université Catholique de Louvain, Louvain-La-Neuve, Belgium

(23. II. 1982)

Abstract. The polarizations, $P_{av} \equiv \langle \mathbf{J} \cdot \boldsymbol{\sigma}_\mu \rangle / J$, and $P_L \equiv \langle \mathbf{J} \cdot \hat{v} \rangle / J$ of the ^{12}B in the reaction $^{12}C(\mu^-, \nu)^{12}B$(g.s.) have been measured *simultaneously*, using the method of selective recoil implantation. Their ratio, R is largely immune to the systematics that affect absolute measurements of P_{av} and P_L, more dependent on the dynamics than either, and almost insensitive to corrections for capture to excited ^{12}B states. Our result, R(g.s.) $= -0.512(41)$, yields to $g_P/g_A = 9.0(1.7)$ (impulse approximation) and $F_P/F_A(q^2) = -1.01(14)$ (elementary particle treatment), to be compared to PCAC predictions of 7 and -0.99 respectively. Thus PCAC is quantitatively verified. The neutrino helicity is found to be $h_{\nu_\mu} = -1.06(11)$.

1. Introduction

Since the pioneering work of Godfrey [1], ^{12}C served with its isotopic partners ^{12}B and ^{12}N as a powerful tool to study the semileptonic interaction, both in β-decay and in muon capture. The latter process is even today of considerable importance, since the contributions of the 'induced couplings' (e.g. weak magnetism, pseudoscalar coupling etc.) are as a consequence of the large momentum transfer sizeable as compared to the allowed axial term. The relative magnitude of the pseudoscalar contribution, inaccessible in β-decay and quantitatively predicted through the PCAC hypothesis, is particularly interesting, since the available experimental information is still rather limited.

In this paper we describe a series of experiments in which the polarization of the ^{12}B recoil nuclei is measured quantitatively. These experiments provide a novel method for the study of the dynamics of muon capture and furthermore yield an accurate determination of the muon neutrino (ν_μ) helicity.

There arise actually two different types of polarization of the ^{12}B recoil nucleus ($J = 1$). First, there is a longitudinal polarization, P_L, i.e. a polarization of recoil along its direction of flight; this is a parity-violating effect. Second, there is a so-called average polarization, P_{av}, i.e. a polarization of the recoil nucleus along the spin of the muon at its instant of capture. This is a parity-conserving quantity.

Both polarizations are measured via the up-down asymmetry in the decay of polarized ^{12}B, exploiting the fact that there exist implantation materials in which the polarization is substantially retained (at least in the presence of an external 'holding' field) for several boron mean lives (~30 msecs). A measurement of P_{av} has already been performed along these lines by the Louvain–Saclay–ETHZ collaboration [2], using a homogeneous graphite target.

The longitudinal polarization or, equivalently, the neutrino helicity, cannot be determined without distinguishing a recoil direction ($\hat{v}$) from its opposite ($-\hat{v}$). We achieved this by the technique of 'selective implantation', which can be explained as follows. Consider the space surrounding the point of recoil production divided into two arbitrary hemispheres. Let one of these hemispheres be a polarization preserving medium, and the other a polarization relaxing one, a situation which can be realized by a proper choice of the two materials. Thus the observed polarization originates only from recoils into a *specified* hemisphere. In practice, the recoils are produced in a thin carbon layer, sandwiched between a depolarizing and polarization retaining layer. Conceptually, the experiment is the muonic analogue of the celebrated Goldhaber–Grodzins–Sunyar [3] experiment on the helicity of the electronic neutrino. Both involve in fact identical spin sequences ($0 \rightarrow 1 \rightarrow 0$). The helicity of the muonic neutrino has been investigated previously by analyzing the muon polarization from π-decay with electromagnetic methods [4]. Those experiments served only to fix the sign of the helicity. The present work yields an accurate determination, and provides a nice 'lecture demonstration' of parity violation.

In the present experiments, P_L and P_{av} are measured simultaneously. One thus not only obtains more accurate data on P_{av} which confirm the results of Ref. 2, but has three additional advantages, viz. (a) the ratio $R = P_{av}/P_L$ is more sensitive to the dynamics than either polarization, (b) all difficulties connected with *absolute* recoil polarization measurements are circumvented, and (c) the corrections for excited ^{12}B states (formed in 10% of all captures) are smaller for R than for P_{av} alone.

In Section 2 we derive the requisite theoretical expressions for the observables, Section 3 explains the principle of the measurements. Section 4 describes the details of the experimental procedure. In Section 5 we present the final results and finally Section 6 contains the discussion and a summary of the relevant data.

2. Observables in the reaction $^{12}C(\mu, \nu)^{12}B$

The μ-capture reaction $^{12}C(\mu, \nu)^{12}B$ is well suited to study both the neutrino helicity and the induced terms of the axial current for the following reasons:

(i) The magnitudes of the 'induced' terms in semileptonic weak interactions are proportional to the momentum transfer, which is high in μ-capture reactions (0.74 m_μ^2).

(ii) The ground state capture in ^{12}C is a pure (non-relativistic Gamov-Teller) transition between well defined states. The ^{12}B daughter nucleus is predominantly (88% [5, 19], see Fig. 1) formed in the ground state.

(iii) The β-active daughter nucleus (^{12}B, $\tau = 29.4$ msec) offers the possibility of measuring its polarization through the up-down β-decay asymmetry.

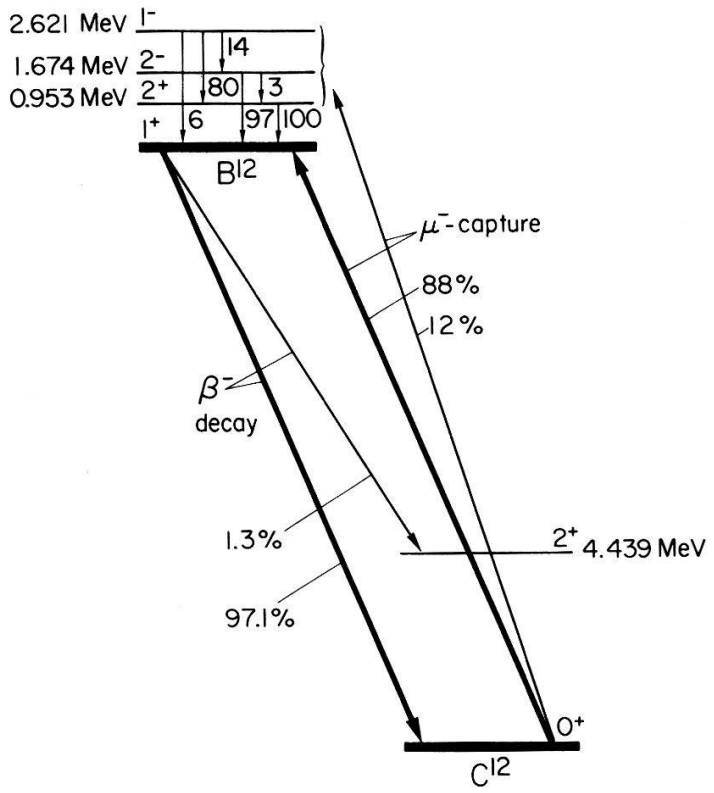

Figure 1
Relevant data for μ-capture on ^{12}C resp. β-decay of ^{12}B.

As polarizations are ratios of matrix elements, the nuclear physics complications generally cancel in first approximation. Polarization measurements are therefore a strong tool for investigating the nature of weak interaction.

(iv) A sufficient number of well-defined observables (e.g. β-decay asymmetry coefficients α_-, α_+) in related transitions in the $A = 12$ triad are available to extract the relevant form factors rather uniquely. This is particularly true for the 'induced' pseudoscalar piece of the current which, as is well known, does not intervene appreciably in β-decay.

If time reversal invariance holds, this reaction is described by three real parameters, corresponding to the description of the spin $\frac{1}{2}$ initial state. If, in addition, the neutrino helicity is assumed to be -1, only two parameters remain. The observables which correspond to these parameters are the capture rate (Γ_μ), the longitudinal (P_L) and the average (P_{av}) polarization, defined as:

$$P_L = \langle \mathbf{J}\hat{v}\rangle/J$$
$$P_{av} = \langle \mathbf{J}\hat{P}_\mu\rangle/J \tag{2.1}$$

where $\hat{v}$ = recoil direction, $\hat{P}_\mu$-direction of muon polarization and $\mathbf{J}$ = nuclear spin.

These observables will be computed in what follows (for a detailed discussion see also Ref. 6). Since the muon is captured from a ^{12}C nucleus at rest, the neutrino and ^{12}B recoil are emitted opposite to each other. We consider two reference frames (Fig. 2): one frame (z') is the ^{12}B recoil frame with the z'-axis parallel to $\hat{v}$, the other is the muon frame (z) with the z-axis taken along the muon polarization P_μ. To calculate the polarization $P'(\theta)$, θ being the angle

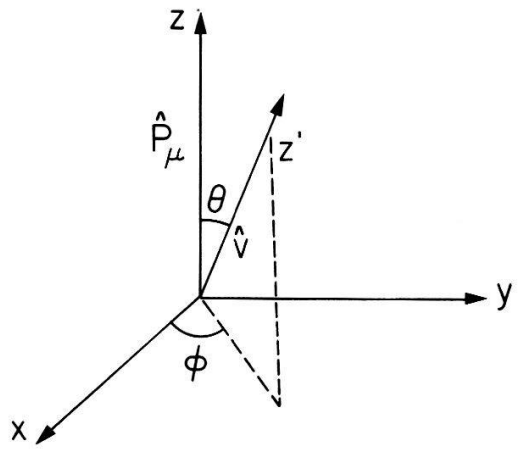

Figure 2
Muon frame ($z \parallel$ muon polarization $\hat{P}_\mu$) resp. recoil frame ($z' \parallel$ recoil direction $\hat{v}$).

between $\hat{P}_\mu$ and $\hat{v}$, let us write the reaction in the following way:

$$\mu^- + \bar{\nu}_\mu + {}^{12}\mathrm{C} \rightarrow {}^{12}\mathrm{B} \tag{2.2}$$

To be specific, let us assume the ν_μ-helicity (h_ν) to be -1 and the muons to be fully polarized ($P_\mu = 1$). In the z'-frame one has then $|\bar{\nu}\rangle' = |\frac{1}{2}, -\frac{1}{2}\rangle$ and for the muon:

$$|\mu\rangle' = \cos(\theta/2)\,|\tfrac{1}{2}, \tfrac{1}{2}\rangle' + \sin(\theta/2)\,|\tfrac{1}{2}, -\tfrac{1}{2}\rangle' \tag{2.3}$$

The corresponding spin state of ^{12}B is the direct product of $\bar{\nu}$ and μ-states with the transition operator (with amplitudes M_0 and M_-) applied:

$$|B(\theta)\rangle' = M_0/\sqrt{2}\cos(\theta/2)\,|1, 0\rangle' + M_- \sin(\theta/2)\,|1, -1\rangle' \tag{2.4}$$

From this state one gets the polarization in the recoil system by forming:

$$P'_i(\theta) = {}'\langle B|\, J_i\, |B\rangle' \quad \text{for} \quad i = x, y, z \tag{2.5}$$

and the capture rate to the ^{12}B(g.s.) will be:

$$\Gamma_\mu = M_0^2/2 + M_-^2 \tag{2.6}$$

If $P_\mu \neq 1$, the state $|B(\theta+\pi)\rangle'$ has to be incoherently added, similarly if $h_\nu \neq 1$ the M_+-state will also be populated and must be added. For the polarization in the recoil system (z') one obtains:

$$\begin{aligned} P'_x(\theta) &= (2/\Gamma_\mu) P_\mu \cdot \sin\theta \cdot \mathrm{Re}\,(M_0^* \cdot M_-) \\ P'_y(\theta) &= (2/\Gamma_\mu) P_\mu \cdot \sin\theta \cdot \mathrm{Im}\,(M_0^* \cdot M_-) \\ P'_z(\theta) &= (M_-^2/\Gamma_\mu) \cdot (h_\nu + P_\mu \cdot \cos\theta) \end{aligned} \tag{2.7}$$

One gets the polarization in the muon-system (z) by rotating the polarization vector equation (2.7) by $-\theta$ and ϕ and averaging over the unphysical angle ϕ so that $P_x(\theta)$ and $P_y(\theta)$ vanish, and gets:

$$P_z(\theta) = P'_z(\theta)\cos\theta + P'_x(\theta)\sin\theta \tag{2.8}$$

Finally the polarization averaged over all space is:

$$P_\mu P_{\text{av}} \equiv \tfrac{1}{2}\int P_z(\theta)\sin(\theta)\,d\theta$$
$$P_{\text{av}} = (\tfrac{1}{3})\cdot(2\,\text{Re}\,(M_0^*\cdot M_-)+M_-^2)/\Gamma_\mu \tag{2.9}$$

Suppose $h_\nu = -1$ for the following discussion. From equation (2.7) one then sees that the ^{12}B has a finite polarization (in its direction of flight) even if $P_\mu = 0$; this is the longitudinal polarization, i.e.

$$P_L = -M_-^2/\Gamma_\mu \tag{2.10}$$

The two polarizations P_L and P_{av} supply two different pieces of information since they depend on the absolute value or on the relative phase of the matrix elements respectively.

If there are no induced terms in the interaction (i.e. $q = 0$), then the transition operator M consists of a single term, M_0 and M_- are equal, and P_L resp. P_{av} become fixed numbers:

$$P_L = -\tfrac{2}{3}, \qquad P_{\text{av}} = \tfrac{2}{3} \tag{2.11}$$

The induced terms affect M_0 and M_- differently, and we define:

$$X \equiv M_0/M_- \tag{2.12}$$

which characterizes the dynamics of the capture process. If time reversal invariance holds, X is a real number, and P_{av} and P_L are no longer independent:

$$\begin{aligned}\Gamma_\mu &= C(2+X^2)\\ P_L &= -2/(2+X^2)\\ P_{\text{av}} &= \tfrac{2}{3}(1+2X)/(2+X^2)\\ R &= P_{\text{av}}/P_L = -\tfrac{1}{3}(1+2X)\end{aligned} \tag{2.13}$$

We conclude: Under the assumption of ν_μ-helicity to be -1 and time reversal invariance to hold one has two independent variables (X and Γ_μ), and P_{av} and P_L are connected by a quadratic relation. If the ν_μ-helicity is no longer -1, the two observables are independent and P_L is proportional to the helicity.

$$P_L = h_{\nu_\mu}\cdot 2/(2+X^2) \tag{2.14}$$

The dynamical meaning of X will be discussed in Section 6.

3. Principle of measurements

3.1 *Selective implantation*

Let us recall the Goldhaber–Grodzins–Sunyar [3] experiment and compare it to our experiment. The reactions are:

$$\begin{aligned}&^{152}\text{Eu}+e^- \rightarrow {}^{152}\text{Sm}^* + \nu_e\\ &^{12}\text{C}+\mu^- \rightarrow {}^{12}\text{B} + \nu_\mu\\ \text{Spins}\quad &0\ \tfrac{1}{2} \qquad 1\ \tfrac{1}{2}\end{aligned} \tag{3.1}$$

In such experiments, i.e. in determining the helicity of neutrinos, one has to select the direction of flight of the neutrino and to measure its polarization with respect to that direction. Since the neutrino polarizes the daughter nucleus – if it has definite helicity – and makes it recoil, a determination of the ν_μ-helicity is equivalent to the determination of the polarization (P_L) of the daughter nucleus along the recoil direction.

In the electron capture one measured the circular polarization of the γ-radiation emitted by the excited recoil nucleus, and the recoil direction was selected by means of a Doppler effect, namely by resonance fluoresence. In the muon capture the recoil nucleus (^{12}B) is β-active; the up-down decay asymmetry is a measure of its polarization. To understand the selection of the recoil direction consider space as divided into two arbitrary hemispheres, say F (forward) and B (backward). The recoil polarization averaged over the whole space is zero (as no direction is distinguished as long as muons are unpolarized). Mirror symmetry is broken if the recoil polarization averaged over one of these hemispheres (say F) is finite; the average over the other hemisphere (say B) must evidently be equal and opposite. To measure the polarization of the nuclei recoiling into one of these hemispheres, one destroys the polarization of those recoiling into the other; note that nuclear polarization may be retained (or destroyed) according to the material in which the recoils come to rest (see Section 4).

In practice (see Fig. 3), one uses a *PCD*-sandwich consisting of three layers: ^{12}B nuclei are produced by μ-capture in the thin central carbon-layer (C). Let the left-hand layer (P) preserve the polarization of the implanted ^{12}B recoils, and the right-hand layer (D) destroy that polarization. This arrangement yields the polarization of the nuclei recoiling into the F hemisphere; if one flips the sandwich, the polarization of the recoils emerging into B is determined (opposite!). This idea to use a sandwich target to measure the longitudinal polarization was proposed by L. Grenacs et al. [7].

Imagining a mirror plane in the carbon layer of the sandwich, the flipping of the sandwich is equivalent to a mirror transformation. Assuming one has a detector (T_1 or T_2) sensitive to the nuclear polarization (i.e. a detector for β-rays)

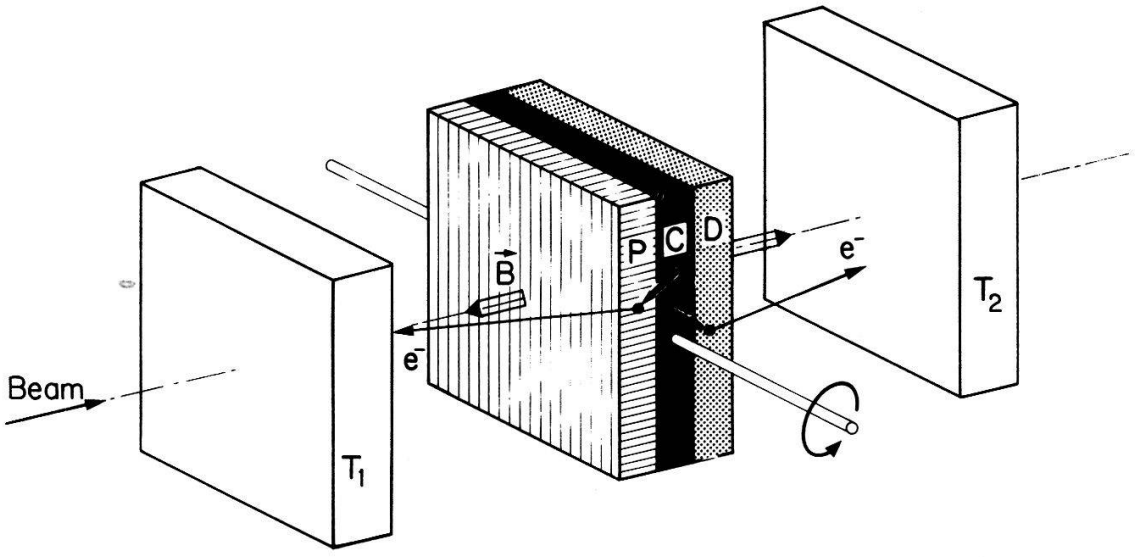

Figure 3
Principle of experiment: *PCD* = stack target (see Text); T_1, T_2 = electron detectors.

one can produce a direct demonstration of parity violation through the change in detector rates between the original and the flipped positions.

In the electron-capture experiment the initial state was unpolarized (Spin zero nucleus and two K-electrons with oppsote spins); as a consequence one had only one measurable polarization, the neutrino helicity or, equivalently, the polarization of the daughter nucleus (P_L). In μ-capture, the recoil-nucleus – if the μ was polarized (P_μ) – could be polarized along the μ-spin ($P_\mu P_{\text{av}}$) even if the emitted neutrino had zero helicity (i.e. if parity was conserved). This offers the interesting possibility of measuring a ratio of polarizations ($P_\mu P_{\text{av}}/P_L$). As this ratio is characteristic for the interaction responsible for the muon-capture (see equation (2.13)), no absolute recoil polarization measurements are required.

3.2 *Polarizations in a sandwich target*

The target was placed perpendicular to the beam and flipped (see above). Its orientation was defined with respect to the component of the muon polarization in the beam direction ($P_\mu \hat{z}$); we used a beam which was 'lefthanded' e.g. $\mathbf{P}_\mu$ is essentially antiparallel to the direction of flight. We define as forward orientation (F) of the target that orientation where the polarization of those nuclei is preserved which recoil along $\mathbf{P}_\mu$, we call backward orientation (B) that in which the recoils opposite to $\mathbf{P}_\mu$ keep their polarization. As the observable polarization is preserved in one hemisphere only, one measures the following quantities (equation (2.8)):

$$\mathbf{P}^F = \frac{\int_F \mathbf{P}(\theta) \sin(\theta)\, d\theta}{\int_{F+B} \sin(\theta)\, d\theta} \tag{3.2}$$

$$\mathbf{P}^B = \frac{\int_B \mathbf{P}(\theta) \sin(\theta)\, d\theta}{\int_{F+B} \sin(\theta)\, d\theta} \tag{3.3}$$

As a function of the two polarizations $P_\mu P_{\text{av}}$ and P_L (equations (2.9, 2.10)) these integrals are:

$$\mathbf{P}^F = \tfrac{1}{2}(P_{\text{av}} \cdot \mathbf{P}_\mu + \tfrac{1}{2} P_L \cdot \hat{z}) \tag{3.4}$$

$$\mathbf{P}^B = \tfrac{1}{2}(P_{\text{av}} \cdot \mathbf{P}_\mu - \tfrac{1}{2} P_L \cdot \hat{z}) \tag{3.5}$$

The axis $\hat{z}$ is opposite to the beam direction. Note that the observable polarizations are attenuated by a factor of two because one hemisphere is depolarizing. Similarly, since P_L is defined with respect to the recoil direction, integration over the hemisphere reduces its observable value by an additional factor of two. As expected, the difference of the polarizations in the two orientations must be proportional to a parity-violating quantity (P_L), and their sum to a parity-conserving one ($P_\mu P_{\text{av}}$); this sum clearly corresponds to a target which preserves polarization over all space (called *PCP*-target). Such a target was constructed to measure P_{av} separately.

Equations (3.4, 3.5) must be slightly amended to allow for the fact that even in the P layers only recoil polarization along a weak external 'holding' field is retained. Obviously, we will apply this field parallel to the beam axis; the result is then:

$$P_\mu = \mathbf{P}_\mu \hat{z}$$
$$P^F = \mathbf{P}^F \hat{z} = \tfrac{1}{2}(P_{\text{av}} \cdot P_\mu + \tfrac{1}{2}P_L) \tag{3.6}$$

$$P^B = \mathbf{P}^B \hat{z} = \tfrac{1}{2}(P_{\text{av}} \cdot P_\mu - \tfrac{1}{2}P_L) \tag{3.7}$$

and the ratio is defined by

$$R \equiv \frac{P^F + P^B}{2 \cdot k \cdot (P^F - P^B)} = P_\mu \cdot P_{\text{av}}/(k \cdot P_L) \tag{3.8}$$

Where k describes the depolarization of muons (due to either beam optics or the cascade mechanism). Note that $P_\mu = -h_{\nu_\mu} k$; the helicity drops out in R.

3.3. *Determination of muon polarization*

Negative muons have lost about $\frac{5}{6}$ of their initial polarization [8] when they reach the ground state of a ^{12}C-atom. This residual polarization can be determined by several methods. We used the time-integral method [9], which allows one to make full use of contemporary meson factory's high muon fluxes, since the incoming muons need not to be separated in time.

The idea is to precess the muon polarization P_μ with an external field B, and to observe the decay electron rate as a function of this B. Assume one observes the decay electrons in the precession plane (perpendicular to B) at an angle θ to the initial muon polarization $\mathbf{P}_0$ (which generally coincides with the beam direction). For convenience, consider this plane as a complex one, with the real axis taken along $\mathbf{P}_0$. For $B = 0$ the counting rate will evidently be proportional to the probability:

$$W(0) = \text{Re} \int_{-\infty}^{0} (1/\tau) \exp(t/\tau) \cdot (1 - P_0 \cdot a \cdot \exp(i\theta))\, dt \tag{3.9}$$

where a is the asymmetry parameter characteristic of muon decay (ideally equal to $\frac{1}{3}$) and τ is muon mean life.

The precession introduces an additional angle γBt, and (3.9) becomes:

$$W(B) = \text{Re} \int_{-\infty}^{0} (1/\tau) \exp(t/\tau)(1 - P_0 \cdot a \cdot \exp(i(\theta - \gamma Bt))\, dt$$
$$= \text{Re}\,[(1 - P_0 \cdot a \cdot \exp(i\theta)) \cdot (1 + i\gamma B\tau)/(1 + (\gamma B\tau)^2)] \tag{3.10}$$

To avoid backgrounds, one will in praxis measure the electron rate at 90° to the incident beam axis, i.e. $\theta = \pi/2 + \delta$, where δ allows for a possible departure of P_0 from that axis. The relevant probability is then:

$$W(B) = 1 - P_0(\gamma B\tau \cdot \cos\delta + \sin\delta)/(1 + (\gamma B\tau)^2) \tag{3.11}$$

The quantity relevant for the experiment is the polarization along the beam axis, i.e. $P_\mu = P_0 \cos\delta$.

4. Experimental procedure

4.1. *Target and implantation studies*

For the construction of the target various constraints had to be observed. The *C*-layer had to be thin enough to let the majority of the recoils emerge (i.e. thinner than 1 μm). This required on one hand a large number of *DCP* layers to have a reasonable ^{12}B production rate and on the other hand the strict avoidance of any carbon containing material in the construction of the setup. Since nuclear spins generally loose their orientation very rapidly when implanted into solids (characterized by the relaxation time T_1) one had to decouple them from local disturbing fields. This decoupling should be as complete as possible in the *P* material and should not take place in the *D* material. Note that *P* layers are also depolarizing in the absence of a magnetic field; thus the physical effect could be switched off by switching off the field! Furthermore, electrons from ^{12}B decay suffer substantial backscattering when passing through more than 0.5 g/cm^2 of high *Z* material; all layers should therefore be made out of low *Z* material and the whole target mass should not exceed 2 g/cm^2.

In order to investigate the relaxation of ^{12}B implanted into various materials, we carried out some separate experiments on the tandem Van de Graff accelerator of ETHZ, where we produced this nucleus by the reaction ^{11}B$(d, p)^{12}$B at $E_d = 1.45$ MeV. The recoils had about the same energy as those in the μ-capture reaction (380 keV). This implantation method was first introduced by L. Madansky [10] and was further investigated in Louvain-la-Neuve [2] as well as at ETHZ. We used the setup described in Ref. 11, with the same bombardment/observation sequence as in the μ-capture experiment (30 ms/60 ms). For each value of the holding field, the residual polarization $P(T_P + T_W)$, i.e. the polarization at the beginning of the measuring period (see Fig. 7), and its relaxation were analyzed by substracting spectra taken with field (ON) from those without field (OFF): the resultant spectra, showing directly the polarization as a function of time, were fitted with an exponential $P(t) = P(T_P + T_W) \exp(-t/T_1)$. Once the relaxation time T_1 is thus known, one corrects the measured polarizations to its initial value $P(0)$, at time $t = 0$ according to:

$$P(T_P + T_W)/P(0) = \frac{\lambda[1 - \exp(-LT_P] \exp(-LT_W)}{L[1 - \exp(-\lambda T_P)] \exp(-\lambda T_W)} \tag{4.1}$$

where T_P = production, T_W = waiting, T_0 = observation time, T_1 = relaxation time, $1/\lambda = \tau = 29.4$ msec = mean life of ^{12}B and $L = \lambda + 1/T_1$.

In the μ-capture experiment only the polarization $P(T_P + T_W + T_0)$ is relevant and the correction due to the relaxation may be calculated according to:

$$P(T_P + T_W + T_0)/P(0) = \frac{\lambda^2 \cdot [1 - \exp(-LT_P)] \exp(-LT_W)[1 - \exp(-LT_0)]}{L^2 \cdot [1 - \exp(-\lambda T_P)] \exp(-\lambda T_W)[1 - \exp(-\lambda T_0)]} \tag{4.2}$$

Among the numerous materials investigated, we present the results for those which are well suited to construct a stack target fulfilling the criteria stated above. Since we used exactly the same time structure of production and observation as in the μ-capture experiment, the polarization $P(T_P + T_W + T_0)$ (Fig. 4) is sufficient to

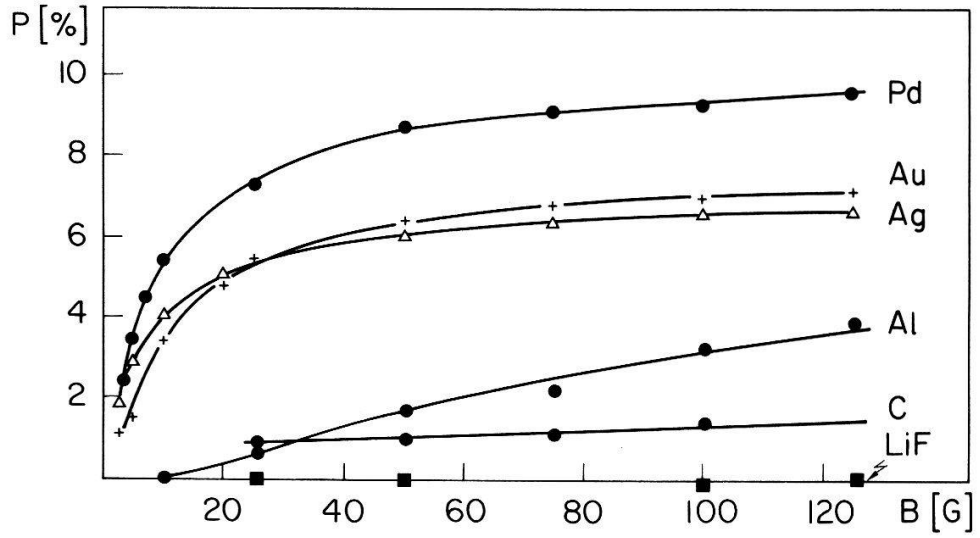

Figure 4
Polarization of ^{12}B produced by $^{11}B(d, p)^{12}B$ reaction after implantation into different materials as a function of the **B** field.

decide which materials are most suited. The attenuation of polarization is only needed for the determination of the magnitude of the neutrino helicity, i.e. for P_L. For the evaluation of X it is not needed since the attenuation drops out in the ratio (R) of polarizations (equation 3.8). To get further insight into the mechanism of relaxation, we measured the relaxation times T_1 as a function of the holding field B (Fig. 5) In Fig. 6 the observed polarizations (from Fig. 4) are corrected for relaxation according to equation (4.2). Two facts can be observed; first the corrected polarizations are not constant as one might expect, but tend to a saturation value and second they reach that value in different ways (e.g. Ag and Au at higher fields (1 kG) only [2]). These two facts can be explained as follows: The hyperfine interaction betweeen the nuclear spin and the spin of unpaired electrons (^{12}B recoils are ionized) depolarize the ^{12}B spin during its flight to the catcher. At high fields one reaches the Paschen-Back region. There occurs furthermore a very rapid relaxation mostly due to quadrupole interaction, which cannot be seen in our time spectra.

We assume that the polarizations measured in Pd and corrected for relaxation are the true polarizations of ^{12}B at the instant of implantation. To know the attenuation factor for a given material and field one must therefore compare the curves in Fig. 4 with the Pd curve in Fig. 6.

The influence of backscattering on the observed polarizations was investigated by varying the thickness of the implantation catcher. The measurements were done for three materials (Pb, Ag, Al) and yielded for the actual target a polarization attenuation of 1.61(12). Extrapolating the backscattering result of Ref. 2 obtained at low Z one gets 1.89(20). Averaging these two results, one obtains an attenuation factor of 1.68(10). Note that the $^{11}B(d, p)^{12}B$ experiment cannot reproduce the situation in μ-capture exactly since the backscattering layer was not normal to the telescope axis but tilted at 45°.

To construct the *DCP* target, one thousand 1.5 μ thick Aluminum foils were covered by evaporation with 60 $\mu g/cm^2$ C and thereupon with 1200 $\mu g/cm^2$ of Ag, denoted Al/C/Ag. Thus the target consisted of 3000 layers with an overall mass of 1.8 g/cm^2. A second target was made out of 1500 LiF/C/Ag sandwiches

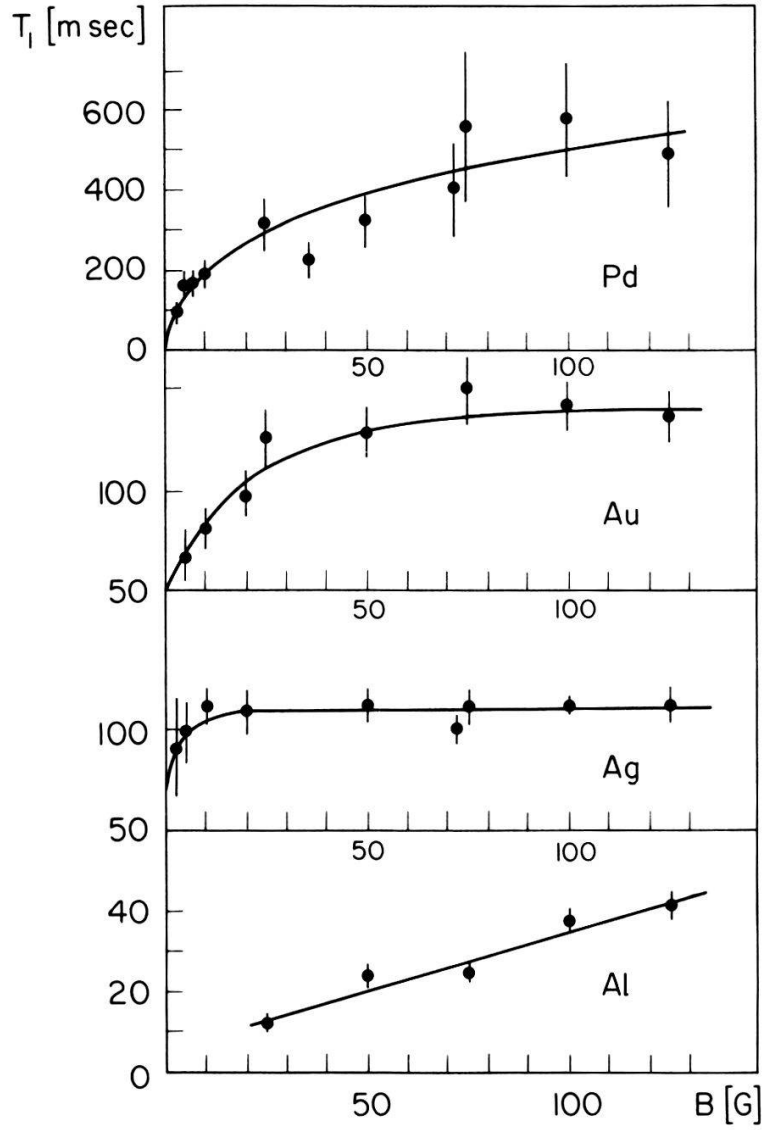

Figure 5
Relaxation times T_1 for the polarization of ^{12}B implanted in several materials.

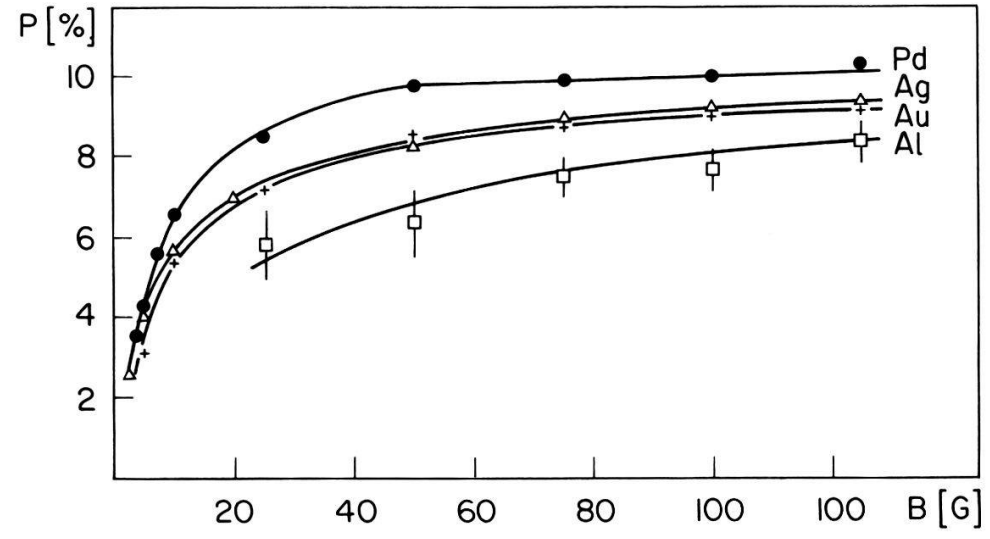

Figure 6
^{12}B polarization from Fig. 4 after correction for the relaxation.

with the masses 250/60/800 $\mu g/cm^2$, denoted LiF/C/Ag. Corresponding $(CH_2)_n$, 'dummy' (*DP*) and nondepolarizing (*PCP*, denoted Ag/C/Ag) targets were also constructed for calibration purposes. The layer structure of the target was analyzed by electron microscopy to ascertain that the layers did not diffuse into each other.

4.2. *Setup*

The experiment was carried out in the μE4 area of SIN at the muon channel II. The channel was tuned for 'backward' muons ($p_\mu = 88$ resp. 70 MeV/c). Typical measuring conditions are given in Table 1. The fact that ^{12}B has a very long mean life (29.4 msec) compared to that of muons in carbon (2 μsec) enables one to measure the ^{12}B activity in the absence of the incident beam. The beam was chopped mechanically by means of two equal counterrotating stainless steel wheels (1.30 m diameter and 5.5 cm thick each). They were cut at two places so that 5.6 rps provided an ON/OFF period of 30 msec/60 msec. The large diameter of the wheel gave a sharp cutoff of the beam (1 msec). Under the actual beam conditions, the chopper suppressed charged particles at the target site by 5.5×10^4.

Since the overall carbon content in the target was only 90 resp. 60 mg/cm^2, the telescopes had to be essentially carbon-free. We used MWPC's with aluminium frames and a 'semi magic' gas mixture (Ar: 94%, isobutane: 6%, freon: 0.1%). They were operated at a voltage of about 2900 V, which was dropped during the 'beam on' period by 500 V to reduce space charge accumulated with beam. To select events coming from the target, the latter was sandwiched between two chambers in anticoincidence (1, 1′ in Fig. 7); furthermore the efficient areas of the chambers were arranged in such a way as to have the solid angle point at the target. These precautions did however not suppress charged particles coming from outside and stopping in the target. Cu absorbers were introduced between the outer chambers (2 and 3, or 2′ and 3′ respectively in Fig. 7) to discriminate against soft electrons ($E < 4$ MeV). The detector assembly subtended a large solid angle (40%). Two Helmholtz coils (HC) supplied a magnetic field <100 G with a homogeneity <3 mG/cm at the target site. An additional transverse field (3 G), perpendicular to the beam and to the telescope axis, was applied during the OFF period (of the main field) to destroy any

Table 1
Summary of measuring conditions

Run no.	Target	p_μ [MeV/c]	Beam spot [mm^2]	Proton beam [μA]	Rangewidth [g/cm^2]
II	LiF/C/Ag	88	64×48	100	1.8
III	Al/C/Ag	70	64×48	100	1.0
		Stop rate 10^5 [sec^{-1}]	Count rate [sec^{-1}]	*S/B*	*B*-field [G]
II	LiF/C/Ag	5.5	8	1.6	75
III	Al/C/Ag	3.8	5.5	2.0	25

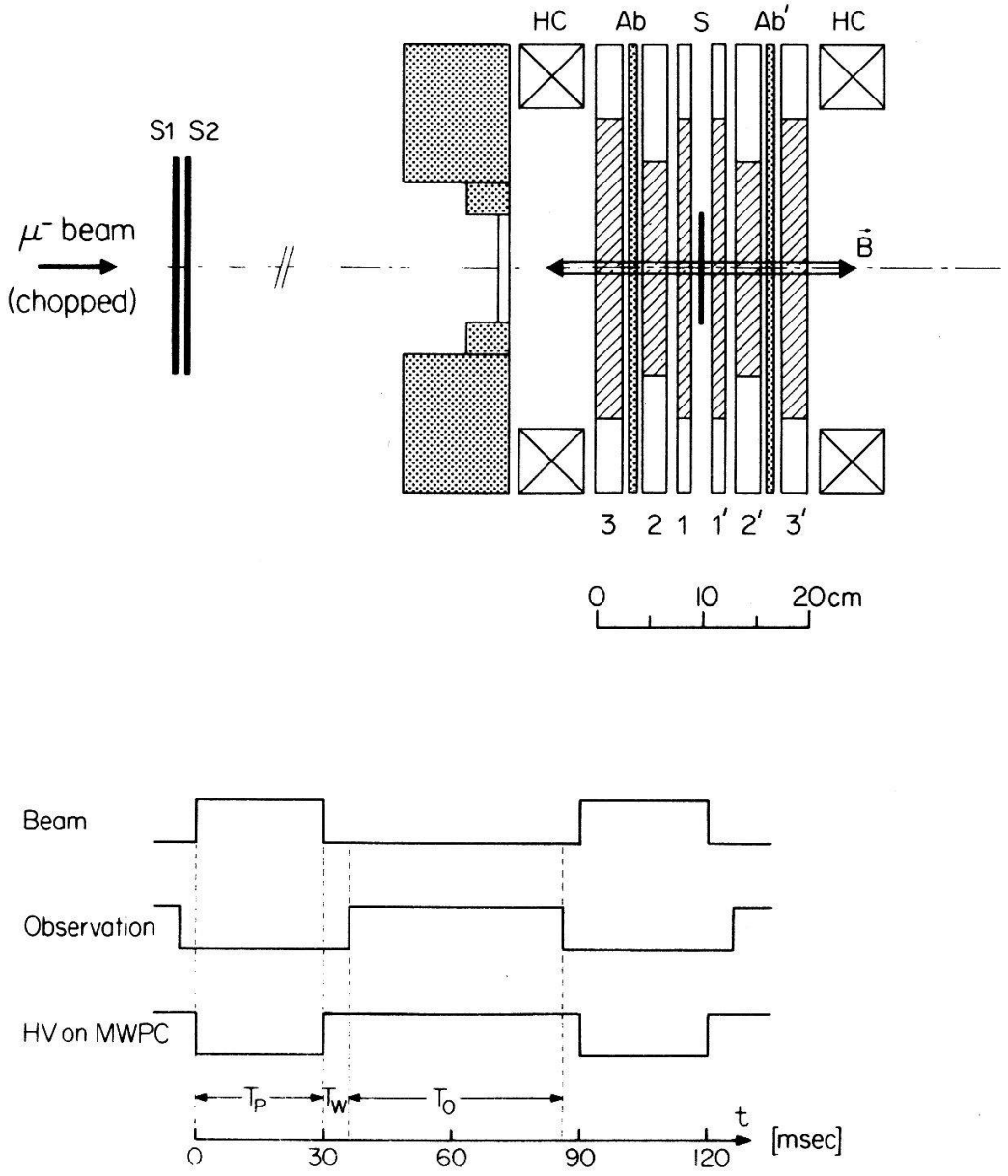

Figure 7
Experimental setup: S = stack target; Ab = absorber; HC = Helmholtz coils; S_1, S_2 = beam monitor; 1, 2, 3 = multiwire proportional chambers and timing diagram: T_p = production, T_w = waiting and T_0 = observation time.

polarization during OFF measurements completely. The sandwich target was flipped by a linear motor device which retracted flipped and repositioned it precisely. The time sequence program was so chosen, that the beam hit the target during 30 msec and was then blocked during 60 msec; 4 msec after cutting the beam the telescopes were ready for counting β-rays during 50 msecs. After every $4 \cdot 10^7$ incoming particles, monitored by two counters S1 and S2, the magnetic field was switched (ON/OFF) and after 10 ON/OFF cycles the target was flipped. This corresponds to one ON/OFF cycle every minute and one target flip every 10 minutes. Good events were defined by $(\overline{S_1 S_2})$ (123) $(\overline{1'2'3'})$ (in Telescope T) and $S_1 S_2$ $(\overline{123})$ 1′2′3′ (in Telescope T'). Such events were stored in a multiscaler with a channel width of 200 μsec. The data aquisition was done with a CAMAC system;

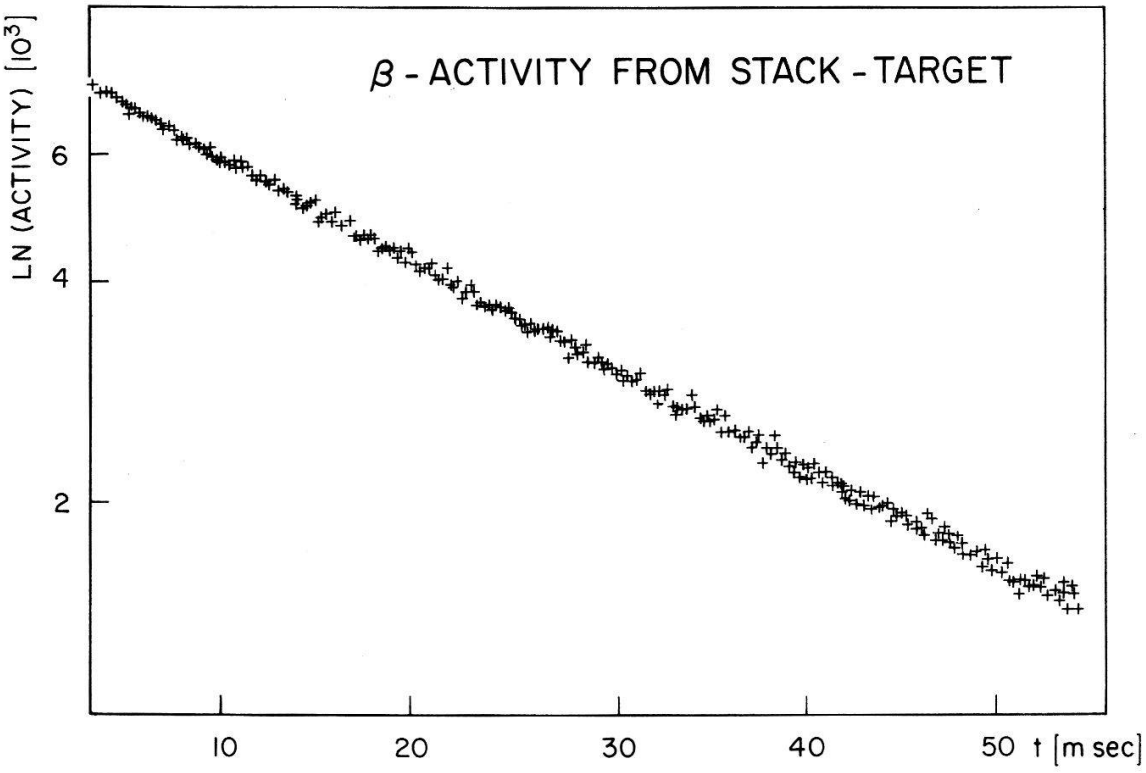

Figure 8
Time spectrum of the ^{12}B decay taken with the stack target containing 60 mg/cm^2 ^{12}C.

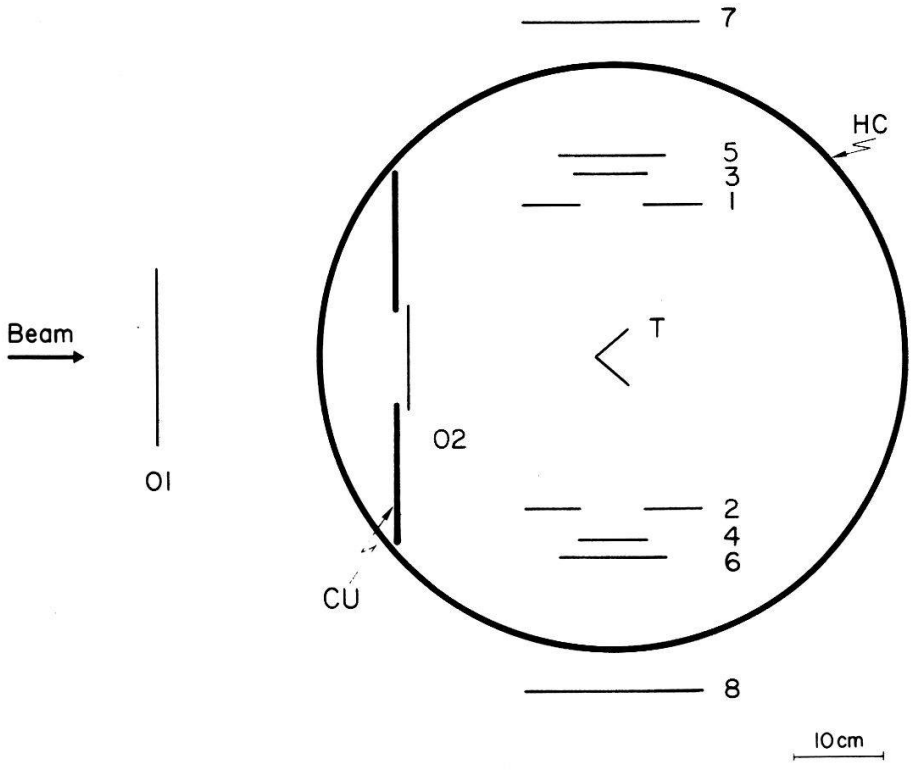

Figure 9
Setup for measurement of muon polarization by Hanle effect method: 01, 02 = beam monitor; HC = Helmholtz coils; T = target; CU = Copper collimator; 1357 resp. 2468 = counter telescopes.

this system generated 8 time spectra, i.e. one spectrum for each telescope, for both field conditions (ON/OFF) and for both target orientations (F, B). A typical time spectrum is shown in Fig. 8 A run lasted about 5 hours, yielding about 20 000 events in each spectrum. The integral assymmetry was about 4% and could be analyzed on line. Data were taken during two measuring periods (Run II and Run III). The measuring conditions are listed in Table 1.

The polarization of the muons (P_μ) was measured in a separate setup but with the same beam conditions used in the measurements of the recoil polarizations. Two telescopes were placed at right angles to the beam (see Fig. 9). The scintillation counters 1357 (for telescope T_1) resp. 2468 (for telescope T_2) were placed in such a way that the incident beam could not hit them directly and that the solid angle (0.8%), defined by the two anticounters (1, 2), subtended exclusively the target. The transverse magnetic precessing field (<100 G) was supplied by a pair of Helmholtz coils. These had 70 cm diameter and a field gradient $dB/dx < 5$ mG/cm over the target region. Residual fields with the main field OFF were compensated by means of three subsidiary pairs of Helmholtz coils (x, y, z) to <10 mG. The target consisted of a butterfly-shaped graphite plate.

5. Results

5.1. *Muon polarization*

P_μ was determined for both momenta ($p_\mu = 88$ resp. 70 MeV/c). Data were also taken with μ^+'s to check the systematics and the analysis procedure. The formula for the counting rate (equation 3.11) must be slightly amended to account for the fact that telescope signals occurring during the first 100 nsec after a muon stop, were rejected (in order to eliminate scattered muons).

$$T_i(B) = I_0 \cdot W(B) = I_0 \cdot [1 - P_0 \cdot a(D \cos\theta + A \cdot \sin\theta)] \tag{5.1}$$

$$T_i(0) = I_0 \cdot W(0) = I_0 \cdot [1 - P_0 \cdot a \cdot \sin\theta] \tag{5.2}$$

where $T_i(B)$ = Rate in telescope $T_1 = (\bar{1}, 3, 5, 7)$ resp. $T_2 = (\bar{2}, 4, 6, 8)$ with magnetic field (B) ON, a = asymmetry parameter characteristic of muon decay, I_0 = stopped muons times solid angle of T_i, $D = \gamma B\tau/[1+(\gamma B\tau)^2]$ (dispersive term), $A = 1/[1+(\gamma B\tau)^2]$ (absorbtive term), $\theta = \delta + \gamma B\,\Delta$, δ = (initial phase of polarization (small), Δ = antigate duration.

Defining the signals $S(B)$ and $P(B)$ in terms of the counting rates T_1 and T_2 as follows:

$$S(B) = \frac{T_1(B)/T_2(B)}{T_1(0)/T_2(0)} - 1$$

$$P(B) = a \cdot S(B)/[S(B)+2] \tag{5.3}$$

one gets by introducing equations (5.1), (5.2)

$$P(B) = (P_0 \cdot a)\frac{(D \cdot \cos\theta + A \cdot \sin\theta) - \sin\delta}{1 - [P_0 \cdot a]^2(D \cdot \cos\theta + A \cdot \sin\theta) \cdot \sin\delta} \tag{5.4}$$

The data points were fitted with the function given in equation (5.4), the free

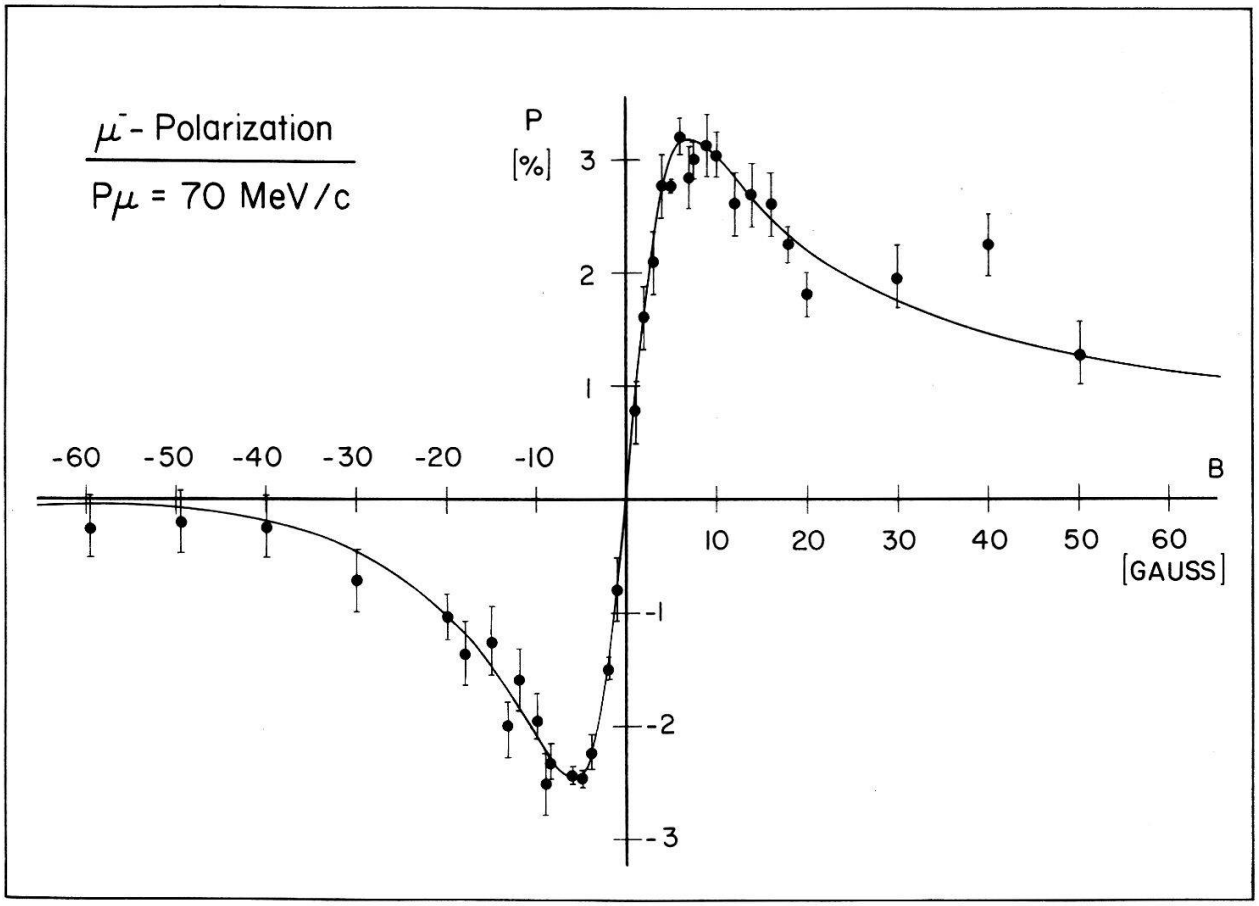

Figure 10
Hanle effect: Measurement of left-right asymmetry as a function of the applied **B**-field.

parameters were beside the quantity (aP_0) the meanlife τ and the misalignment δ. A typical series of measurements of the muon polarization as a function of B is shown in Figs. 10 and 11. With a 100 μA proton beam, 3 hours were needed to collect these data. Background was measured with 'target out', and with an equivalent Pb target. Both measurements, the latter corrected for muons decaying in Pb, yielded a background of 1%. Backscattering of electrons by the target was investigated by backing it with Pb. In addition, its thickness was varied to check whether the energy cut and the backscattering affected the measured polarization. No significant influence could be detected.

The parameter a in equation (5.4) is not known. What is known is the asymmetry parameter α from muons which are not depolarized (measured with μ^+ [12]). This parameter contains the helicity of ν_μ since $P_\mu = -h_{\nu_\mu}$ (for undepolarized muons i.e. $k = 1$). The comparision of the asymmetry $P_0 a = -h_{\nu_\mu} \cdot k \cdot a$ measured in the actual beam and target arrangement with $\alpha = h_{\nu_\mu} \cdot a$ from Ref. 12 yields the atomic and kinematic depolarization factor k (see Table 2).

The fitted $\tau(\mu^+)$ agreed with the literature value, while $\tau(\mu^-)$ was in disagreement with the known value (2.04 μsec [13]). The latter discrepancy can readily be explained in terms of the background observed with 'target out;' it originates from muons stopping in heavy materials (i.e. coils etc.). This background acts as if the target were contaminated with heavy elements (1% of activity coming from Cu can explain the observed reduction).

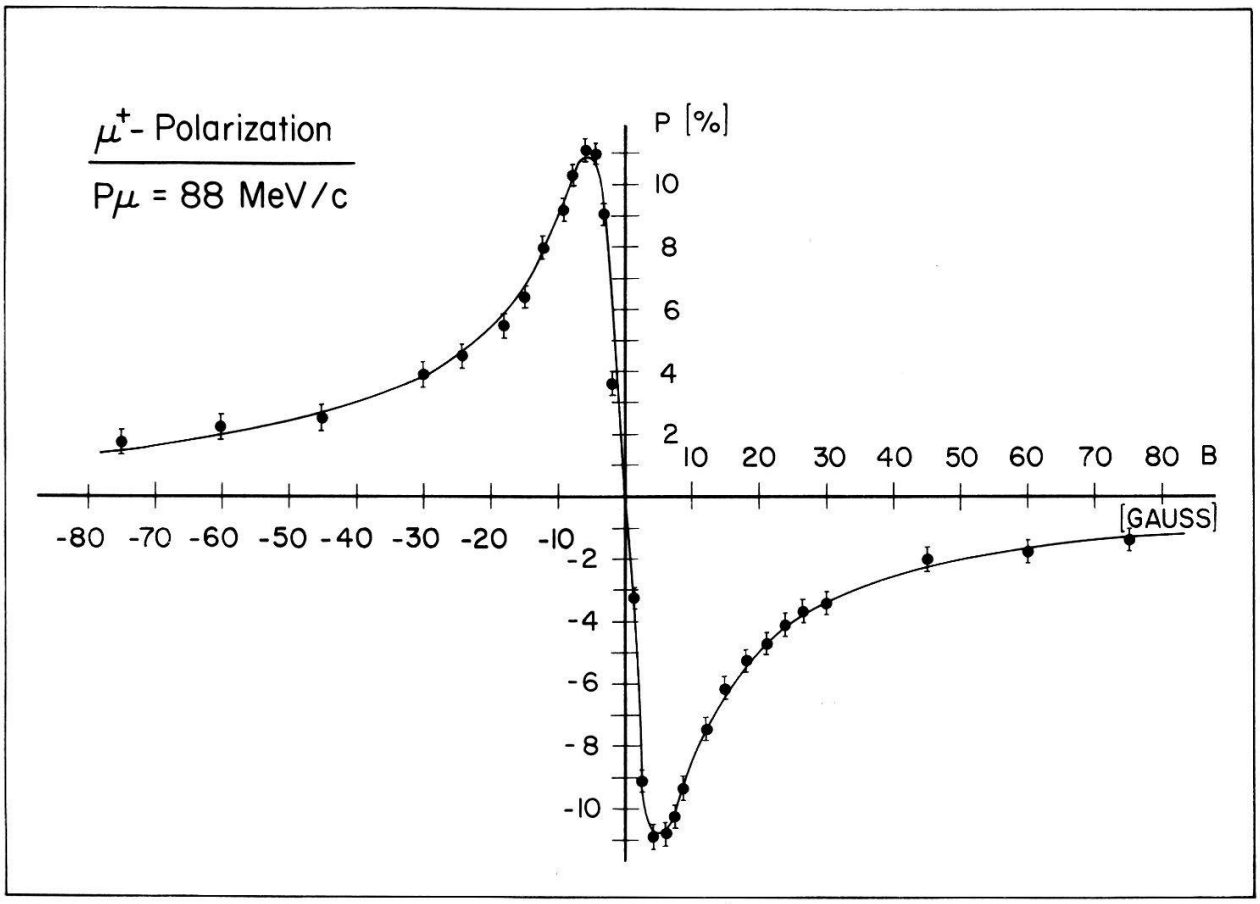

Figure 11
Same as Fig. 10 for μ^+.

Table 2
μ-polarization measurements

p_μ [MeV/c]	target ϕ (cm)	mean life τ (10^{-6} sec)	missalignment δ	Depolarization factor k
μ^+ 88	10	2.22(2)	<1°	0.70(1)
μ^- 88	10	1.78(6)	<1°	0.156(4)
μ^- 70	8	1.74(6)	6(1)°	0.170(4)

From the comparison of measured μ^+ and μ^- polarization one can determine the total depolarization to be:

$$P_{\mu^+}/P_{\mu^-} = 4.5(1), \tag{5.6}$$

in agreement with the literature value 4.7(1) [14].

5.2. *Recoil polarization ratio R*

The procedure for the determination of the raw recoil polarizations was as follows. The time spectra (see Fig. 8) were fitted with an exponential and a flat background, which was assumed to be the same for ON and OFF spectras. For each target orientation B and F and for both telescopes independently one

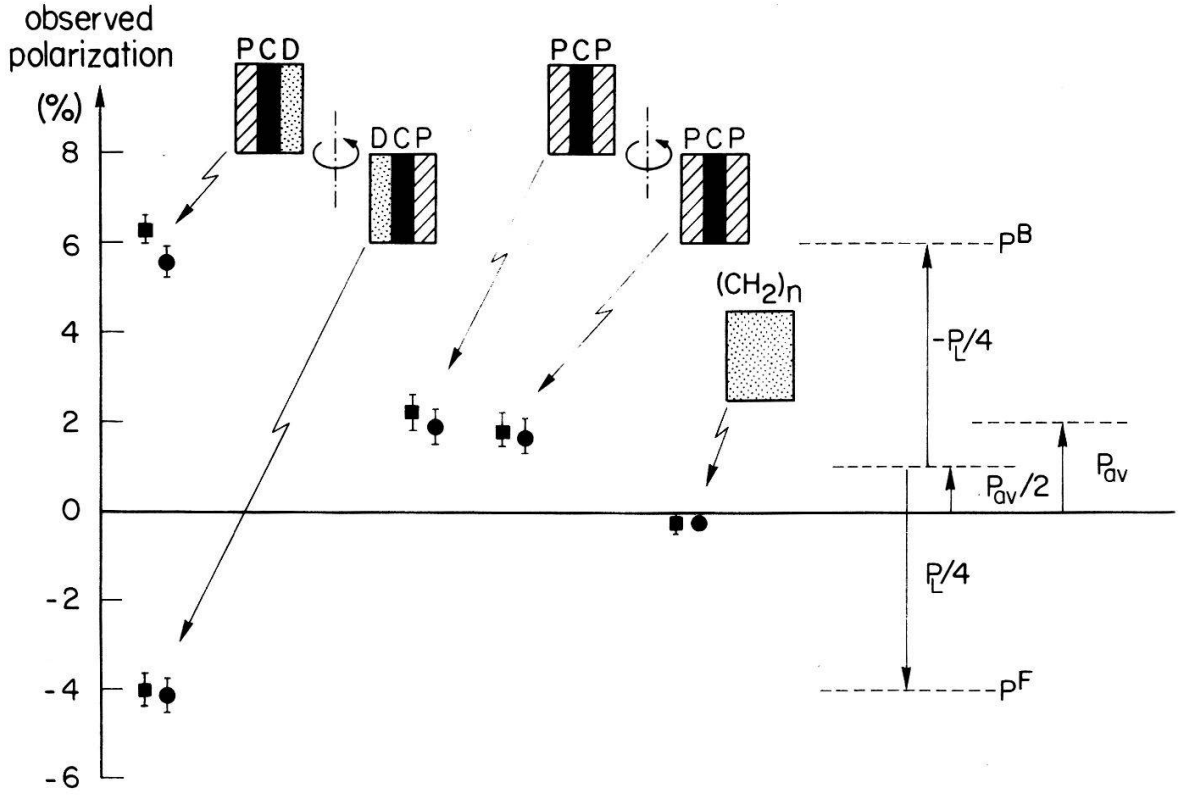

Figure 12
Polarizations observed with various stacks and stack orientations: P = Ag, D = Al; ■ = T_1, ● = T_2. On the right hand side the quantities as defined in equations (3.6), (3.7).

extracted the polarizations by calculating:

$$P^i = -(T^i(B)/T^i(0) - 1) \tag{5.7}$$

where i stands for F or B, $T^i(B)$ is the integral counting rate in one of the telescopes with field B, $T^i(0)$ is the counting rate with the field OFF. The minus sign applies for the fact, that the electrons are preferentially emitted opposite to the ^{12}B polarization.

The raw polarizations (P^F, P^B) measured with the Al/C/Ag target are shown in Fig. 12 (see also Table 3). Clearly the measured polarizations change sign between flipped and original target orientations: Parity violating is manifest! Since most of the corrections cancel in the ratio R (equation 3.8), we correct the raw data only for the following effects which alter this ratio: (a) instrumental asymmetries as measured with the $(CH_2)_n$ depolarizing target (a 0.2% offset), (b) unpolarized background determined as described above (correction factor f = 1.5), (c) ^{12}B coming from sources other than the C layers (f = 1.03). Next we form the quantities ($P^F + P^B$) and $2(P^F - P^B)$ (see Table 4) whose ratio is up to some small calculable corrections equal to kR (see equation 3.8). The results from the

Table 3
Uncorrected measured asymmetries

Target	A^F [%]	A'^F [%]	A^B [%]	A'^B [%]
LiF/C/Ag	1.78(12)	−1.92(12)	−3.75(11)	3.09(11)
Al/C/Ag	2.03(22)	−2.76(22)	−4.61(22)	3.27(22)
Ag/C/Ag	−1.75(27)	0.85(26)	−2.05(27)	0.99(26)

Table 4
Ratio $R = P_{av}P_{\mu}/P_L$

Target	$P^F + P^B$ [%]	$2(P^F - P^B)$ [%]	$(P^F + P^B)/2(P^F - P^B)$	μ-depol. k	R§)
LiF/C/Ag	2.16(27)	−19.02(54)	0.114(15)	0.156(4)	−0.731(97)
Al/C/Ag	1.67(40)	−22.20(90)	0.0834(83)	0.170(4)	−0.491(49)
Ag/C/Ag	1.90(19)	0.53(90)			

§) Note yet correct for finite C-thickness.

Al/C/Ag target must be corrected for incomplete depolarization in the Al-layers, because at 25 Gauss Al still retains 11.1(8)% of the polarization preserved in Ag (see Fig. 4).

The result from the LiF/C/Ag target is clearly in disagreement with that from the other two targets, the ratio R being unreasonably high. This is attributed to the LiF layers which were either not compact or not thick enough and therefore transmitted recoils [15]. Assuming the same P_L in both targets, one can correct for P_{av}, which is statistically not so well determined, and get for LiF/C/Ag $R = -0.523(77)$. The mean result of $R = -0.500(41)$ still has to be corrected for the finite thickness of C-layers and the retention of polarization therein. Since the carbon layers are in practice not infinitely thin, not all ^{12}B recoils can emerge from them, and hence the solid angle over which the polarization has to be averaged is less than 2π. This effect has been evaluated by a Monte Carlo simulation. In the Al/C/Ag target about 20% of all ^{12}B's come to rest in the C-layers. Under the actual measuring conditions, i.e. at a holding field of 75 resp. 25 Gauss, the C-layers retain 10.3(2.0) resp. 11.5(2.0)% (see Fig. 4) of the polarization preserved in the P-layers (out of Ag). This polarization retained in C does not change between F and B orientations of the target and hence contributes to $P_{\mu}P_{av}$. R must be enhanced by 1.032 to allow for these two effects. The mean value becomes then:

$$R(\text{obs.}) = -0.516(41) \tag{5.8}$$

5.3. *Longitudinal polarization* P_L

The measured value $2(P^F - P^B)$ must be corrected for the finite solid angle of electron detection, the thickness of the C-layers and the preservation of polarization in the latter. These corrections (called geom. eff. in Table 5) were evaluated by a Monte-Carlo simulation, yielding altogether 1.53(1). Furthermore this value must be corrected for relaxation in the P layers and for backscattering. Finally there exist some small effects which can produce ^{12}B like activity or dilute the

Table 5
Longitudinal polarization P_L

$2(P^F - P^B)$	Relaxation	Back-scattering	Geometrical effects	Small effects	P_L
−0.222(9)	1.57(2)	1.67(15)	1.53(1)	1.08(1)	−0.96(10)

recoil polarizations (^{13}C content in the target, internal branch of β-decay etc. [2]). The corrections are listed in Table 5, together with the absolute value of P_L, e.g.

$$P_L(\text{obs.}) = -0.96(10) \tag{5.9}$$

5.4. *Corrections for excited states*

The longitudinal polarization P_L (equation (5.8)) and R (equation (5.9)) must be corrected for captures leading to the excited states in ^{12}B. It is worthwhile mentioning from the outset that the uncertainties due to these excited states are well within the statistical errors of P_L and R, and that the effect on R is particularly small, since the corrections largely cancel in this polarisation ratio.

To calculate the corrections the partial capture rates to the excited states ($2^+, 2^-$ and 1^-) as well as their polarizations after μ-capture have to be known. Table 6 summarizes the relevant experimental and theoretical data. As far as the capture rates to the excited states are concerned, they have been remeasured recently [19]; good agreement with earlier determinations occurs only for the sum of the capture rates. The disagreement with the theoretical predictions is particularly striking in the case of Ref. 16 for the 1^--state.

Table 6
Partial capture rates to $^{12}B^*$-states and recoil polarization of $^{12}B^*$

	Experiment			Theory	
	Ref. 5	Ref. 29	Ref. 19	Ref. 16	Ref. 18
1^--state $\Gamma(1^-)[10^3\,\text{sec}^{-1}]$	0.7(4)	0.72(17)	0.38(10)	1.40	0.23
$P_{av}(1^-)$	—	—	$0.6(^{+1}_{-3})$	0.48	−0.25
$P_L(1^-)$	—	—	−0.84(25)	−0.97	−0.62
2^--state $\Gamma(2^-)[10^3\,\text{sec}^{-1}]$	0.4(6)	<0.24	0.12(8)	0.29	0.42
$P_{av}(2^-)$	—	—	—	0.45	0.31
$P_L(2^-)$	—	—	—	−0.40	−0.48
2^+-state $\Gamma(2^+)[10^3\,\text{sec}^{-1}]$	0.2(4)	0	0.27(10)	0.31	0.12
$P_{av}(2^+)$	—	—	—	0.50	−0.29
$P_L(2^+)$	—	—	—	−0.33	−0.29
Bound states $\Gamma(^{12}B^*)[10^3\,\text{sec}^{-1}]$	1.3(8)	0.76(14)	0.77(10)	2.00	0.77

None of the polarizations of the 2^+, 2^- or 1^- state have actually been measured directly and the theoretical predictions do not agree even on the sign. In Ref. 19 we deduced $P_L(1^-)$, since according to Ref. 5 the 1^- state was supposed to make the dominant contribution. Actually the *alignment* of the 1^- state was measured; as the alignment is also a function of X [$A = 2(1-X^2)/(2+X^2)$] $P_L(1^-)$ and $P_{av}(1^-)$ could be deduced and are listed in Table 6.

Table 7
Final result for R and X

R(obs.)	f_R	R(g.s.)	X
Experiment −0.516(41)	—	—	—
Ref. 16	0.98(3)	−0.506(41)	0.26(6)
Ref. 18	1.03	−0.531(41)	0.30(6)
Ref. 16§)	0.97	−0.512(41)	0.26(6)

§) Together with measured capture rates from Ref. 19.

Table 8
Final result for P_L and h_{ν_μ}

P_L(obs.)	f_L	P_L(g.s.)	$(2+X^2)/2$	h_{ν_μ}
Experiment −0.96(10)	—	—	—	—
Ref. 16	1.09(4)	−1.04(11)	1.03	−1.08(11)
Ref. 18	1.06	−1.02(11)	1.05	−1.06(11)
Ref. 16§)	1.06	−1.02(11)	1.03	−1.06(11)

§) Together with measured capture rates from Ref. 19.

In the following we shall give three different correction factors for P_L and R, two based on the theoretical calculations of Refs. 16 and 18, and the third derived using the *measured* partial capture rates, and polarization data for the 1^--state in conjunction with theoretical estimates for the 2^+ and 2^- states. Table 7 presents these correction factors (f_R) for R; the analogous factors (f_L) for P_L are given in Table 8.

5.5. *Final results*

The last column of Table 7 gives the value for X obtained through equation (3.8). The discussion of X, the quantity defined in equation (2.12) and characterizing the dynamics of the μ-capture process, will follow in the next Section.

The determination of h_{ν_μ} is based on the relation (equation 2.14):

$$h_{\nu_\mu} = P_L(2+X^2)/2$$

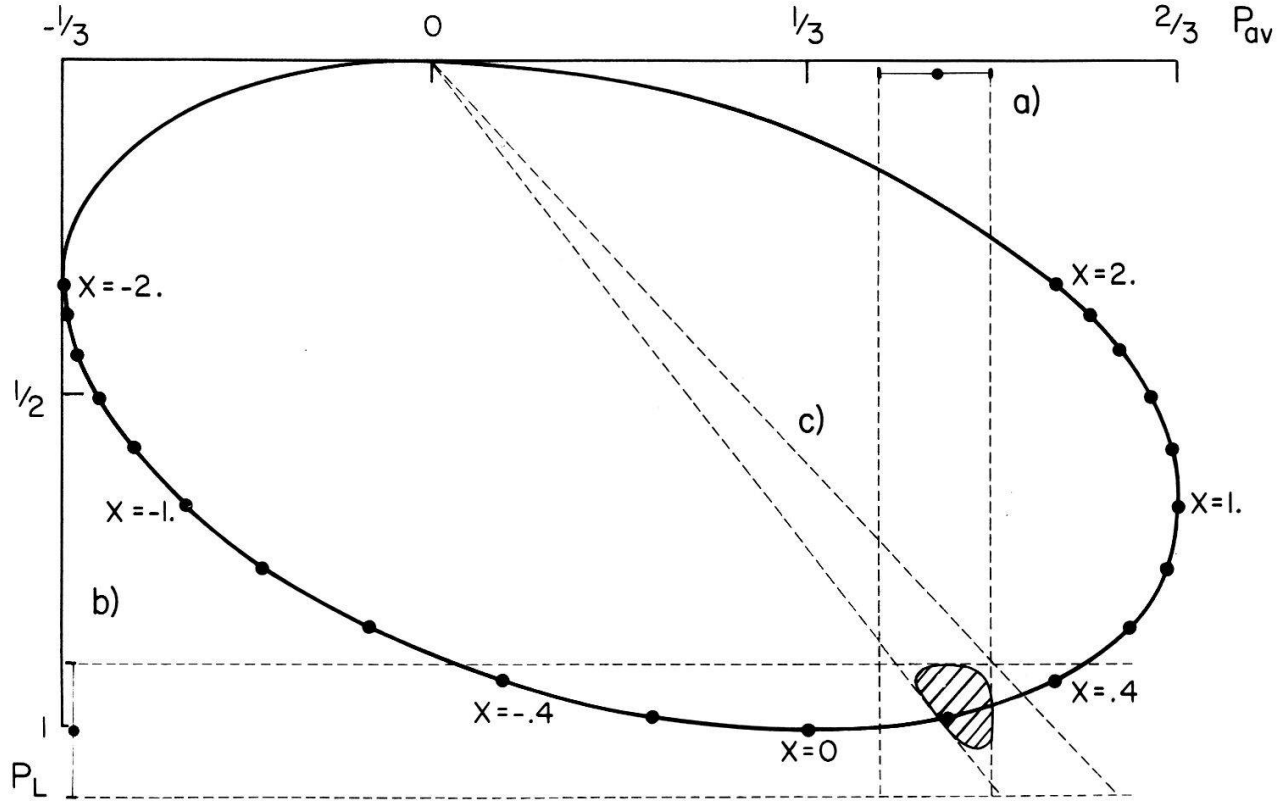

Figure 13
Quadratic relation between P_{av} and P_L; X = ratio of longitudinal to transverse amplitude (equation (2.12)); (a) Ref. 3, (b) and (c) this work.

We note that for the range of interest ($0<X<0.4$) the X-dependence of h_ν is very weak. An experimental value is nevertheless needed; in this work (see Table 8) we used X as determined from the measured R (Table 7). It is also possible, as we did in an earlier publication [15], to use the dependence of the capture rate on X (equation 2.13). While the latter procedure yields $X=0.37(14)$ in agreement with Table 7, it involves additional uncertainties from the q^2-dependence of F_A, and the magnitude of (F_M/F_A).

Using the result of Tables 7 and 8, we can also deduce a new value for the ground state average polarization, namely

$$P_{av}(\text{g.s.})=0.52(7)$$

which is in good agreement with an earlier measurement [2]. This can also be seen in Fig. 13, showing the quadratic relation of P_{av} and P_L, as well as the experimental results.

6. Discussion and conclusions

6.1. *PCAC and pseudoscalar coupling*

In order to describe the dynamical meaning of X two approaches exist, first the 'Elementary Particle Approach' (EPA) [20], and second the 'Impulse or Independent Particle Approach' (IA) [21], describing the interaction of complex nuclei as a super-position of interactions of 'free' nucleons. Note that no second class currents are assumed in what follows, as was experimentally shown [11, 22, 23]. In EPA X is given by:

$$X=\frac{M_0}{M_-}=\frac{F_A+F_P(m_\mu E_\nu/m_\pi^2)-F_E(E_\nu/2m_p)}{F_A+F_M(E_\nu/2m_p)} \tag{6.1}$$

$$=\frac{1+(F_P/F_A)(m_\mu E_\nu/m_\pi^2)-(F_E/F_A)(E_\nu/2m_p)}{1+(F_M/F_A)(E_\nu/2m_p)} \tag{6.2}$$

where the F_i's are form factors taken at $q^2=0.74m_\mu^2$, $i=A=$axial, $P=$ pseudoscalar, $M=$weak magnetic and $E=$1st class weak electric, $m_\mu E_\nu/m_\pi^2=0.4958$, $E_\nu/2m_p=0.04871$. Note that in the 'allowed' limit, in the absence of induced couplings, X is equal to 1.

We see that X is most sensitive to the pseudoscalar form factor F_P ($q^2=0.74m_\mu^2$). Note that only ratios of form factors appear in X (see equation 6.2). In the experiments investigating the correlations between electron momentum and nuclear orientation (α_- and α_+ [11, 22, 23]), the magnitude of $F_M(0)$ and $F_E(0)$ were determined. To compute F_P ($q^2=0.74m_\mu^2$) from X, a weak assumption about the q^2-dependence is needed. We shall follow Primakoff and Hwang [20] and assume that:

$$F_M(q^2)/F_M(0)=F_E(q^2)/F_E(0)=F_A(q^2)/F_A(0) \tag{6.3}$$

This assumption has been confirmed indirectly by Mukhopadhyay and Martorell [21]; however even if it holds to only 20%, the relation between X and F_P is *not*

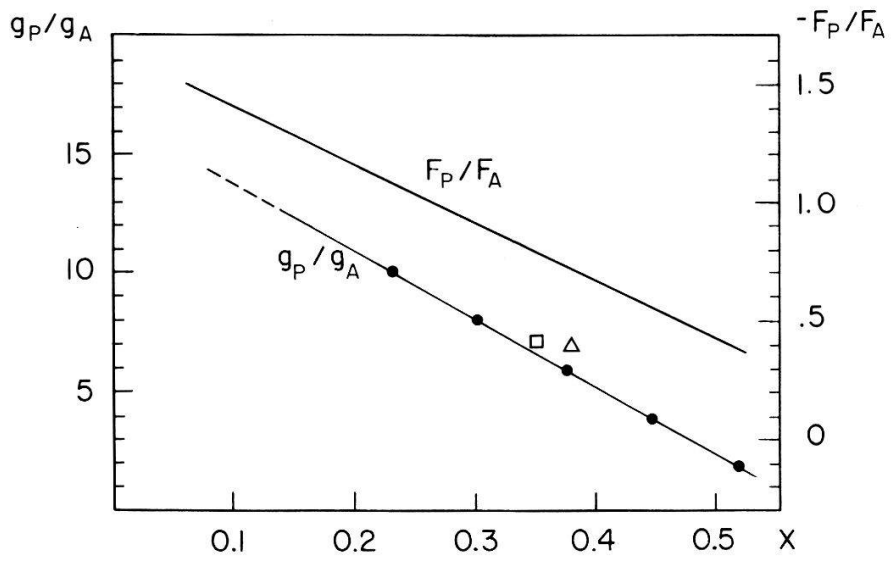

Figure 14
Nucleon resp. nuclear pseudoscalar form factor as a function of X. F_P/F_A from equation (6.4); ○ = Ref. 21, □=Ref. 16, △=Ref. 18.

substantially affected. With the measured values of the form factors, i.e.

$$F_A(0) = 0.512(5)$$
$$F_M(0)/F_A(0) = 3.87(42)$$
$$F_E(0)/F_A(0) = 3.81(42)$$

one gets:

$$F_P(0.74m_\mu^2)/F_A(0.74m_\mu^2) = -1.64 + 2.40X \tag{6.4}$$

(see Fig. 14).

The hypothesis of partially conserved axial vector current (PCAC) [24] gives a prediction of the pseudoscalar form factor $F_P(q^2)$, namely

$$F_P(q^2)/F_A(q^2) = -1/(1 + q^2/m_\pi^2) = -0.71 \tag{6.5}$$

In the elementary particle picture, the validity of PCAC is reduced as π-pole dominance is not expected to hold as well as in the nucleon case [25] and an IPA analysis [17] shows that there are indeed non-pole contributions to F_P, which are usually accounted for by adding a term δ to equation (6.5), $\delta = 0.28$ [17]. PCAC must therefore be suitably corrected, and F_P is predicted [17] to be:

$$F_P(0.74m_\mu^2)/F_A(0.74m_\mu^2) = -0.99 \tag{6.6}$$

In the 'Independent Particle Approach' several authors [21] give a prediction of X on the basis of the 'canonical' values of the weak nucleon form factors; 'canonical' means the values of the form factors as predicted by the symmetry principles CVC, PCAC and G-invariance, the latter as applied to the nucleons rather than to the nuclei as in the 'Elementary particle treatment'. The results of these calculations are shown in Fig. 14. As one can see, X is almost independent of nuclear models. This fact reflects an important advantage of polarization data, i.e. that the latter depend only on ratios of matrix elements. From PCAC one expects

Table 9
Comparision of experiment and theory

Measured X	Experiment g_P/g_A (Fig. 14)	Experiment F_P/F_A Equation (6.4)	PCAC-Prediction g_P/g_A	PCAC-Prediction F_P/F_A
0.26(6)	9.0(1.7)	−1.01(14)	7	−0.99

for the nucleon pseudoscalar form factor

$$g_p/g_A = 7 \tag{6.7}$$

In Table 9 we compare theory and experiment, adopting the calculations of Ref. 21 in the IA treatment, and the calculations of Ref. 17 for the Elementary Particle Approach. We emphasize that the indicated error for the pseudoscalar form factor is mainly given by the statistical uncertainty in R (equation (5.8)), the contribution of the capture to the excited states being of minor importance.

The values of the ratios of pseudoscalar to axial vector form factor extracted from the experiment, are in IA (9.0(1.7)) or in EPA (−1.01(14)), and agree nicely with the PCAC predictions of the two approaches (7 and −0.99 respectively).

6.2. *Neutrino helicity*

Although the $V-A$ theory for weak semileptonic processes has reached its present acceptance through many quantitative agreements between predictions and experiments, it is still esthetically desirable to measure neutrino helicities as directly as possible. For ν_e this was done in the well-known Goldhaber–Grodzins–Sunyar [3] e-capture experiment. In the past, the helicity of the $\bar{\nu}_\mu$ was generally determined by measuring that of the μ in the π decay using the electromagnetic interaction, such as Mott or Møller scattering.

Table 10 summarizes earlier determinations of muon neutrino and antineutrino helicities. One can see that the result of the present work based on the longitudinal polarization of ^{12}B after μ-capture provides the most precise direct determination of the helicity, namely $h_\nu = -1.06(11)$, while the former P_{av}-measurement [2] has given up to now the most accurate antineutrino helicity, namely $h_{\bar{\nu}_\mu} = +1.0(1)$, with only mild and by now well secured assumptions about the capture dynamics.

In conclusion we may say that the $A = 12$ system has turned out to be a powerful tool for the investigation of the weak interaction. In recent years correlation and polarization measurements have provided accurate determinations

Table 10
Muon-neutrino helicity

Experiment	ν_μ	$\bar{\nu}_\mu$
Ref. 26		1.1(4)
Ref. 27		1.17(32)
Ref. 28		~1.0(2)
Ref. 2		1.0(1)
This work	−1.06(11)	

Table 11
Observables and form factors

Observables		Form factors
$\alpha_- = 0.13(12)/\text{GeV}$ $\alpha_+ = -2.73(27)/\text{GeV}$	Ref. 11, 22, 23	
$\Gamma_\mu = 6050(270)\ \text{sec}^{-1}$	Ref. 2	$F_M/F_A(0) = 3.87(42)$
$P_{av}(\text{obs.}) = 0.46(4)$	Ref. 2	$F_E/F_A(0) = 3.81(42)$
$P_{av}(\text{g.s.}) = 0.47(4)$		$F_P/F_A(q^2) = -1.01(12)$
$P_L(\text{obs}) = -0.96(10)$ $P_L(\text{g.s.}) = -1.02(11)$	this work	
$R(\text{obs.}) = -0.516(41)$ $R(\text{g.s.}) = -0.512(41)$	this work	

of the relevant observables in β-decay and μ-capture (see Table 11). The present work having provided a quantitative determination of the pseudoscalar coupling constant, which was the last open question in this field, all the form factors are well established to about 10–15% accuracy and the validity of CVC, PCAC and the absence of SCC has been established.

Acknowledgement

We gratefully acknowledge the efficient assistance of the technical staff of the Laboratories for Nuclear Physics of our two institutions and of SIN.

REFERENCES

[1] T. N. K. Godfrey, Princeton University thesis, 1954 (unpublished).
[2] A. Possoz, Ph.D. thesis, Univ. Catholique de Louvain, Louvain-la-Neuve (1978), unpublished; A. Possoz et al., Phys. Lett. *70B* (1977) 265.
[3] M. Goldhaber et al., Phys. Rev. *109* (1958) 1015.
[4] A. I. Alikanov et al., JETP *11* (1960) 1380, G. Backenstoss et al., Phys. Rev. Lett. *6* (1961) 415, U. Bardon, Phys. Rev. Lett. *7* (1961) 23.
[5] G. H. Miller et al., Phys. Lett *41B* (1972) 50.
[6] V. Devanathan and P. R. Subramanian, Phys. Lett. *53B* (1974) 21; J. Bernabeu, Phys. Lett. *55B* (1975) 313.
[7] L. Grenacs and L. Palffy, Université Catholique de Louvain, Louvain-la-Neuve, internal report (1968).
[8] A. O. Weissenberg, *Muons*, North Holland, Amsterdam (1967).
[9] A. Possoz et al., Phys. Lett. *87B* (1979) 35.
[10] J. J. Berlijn et al, Phys. Rev. *153* (1967) 1152; L. Pfeiffer and L. Madanski, Phys. Rev. *163* (1967) 999; R. L. Williams et al., Phys. Rev. *C2* (1970) 1219.
[11] H. Brändle et al., Phys. Rev. Lett. *40* (1978) 306; H. Brändle et al., Phys. Rev. Lett. *41* (1978) 299.
[12] I. I. Gurevich et al., Phys. Lett. *11* (1964) 185; A. M. Sachs and A. Sirlin, *Muon Physics*, Academic Press, New York (1975).
[13] N. C. Mukhopadhyay, Phys. Reports *30* (1977).
[14] V. S. Evseev, *Muon Physics*, Academic Press, New York (1975).
[15] P. Truttmann et al., Phys. Lett. *83B* (1979) 48; Errata Phys. Lett. *103B* (1981) 469.
[16] M. Kobayashi et al., Nucl. Phys. *A312* (1978) 377; H. Ami et al., Osaka preprint (1980).
[17] W-Y. P. Hwang, Phys. Rev. *20C* (1979) 805.
[18] S. Ciechanowicz, Inst. of Theoretical Physics, Wroclaw, Poland (private communication).
[19] L. Ph. Roesch et al., Phys. Lett. *107B* (1981) 31.

[20] C. W. KIM and H. PRIMAKOFF, Phys. Rev. *139B* (1965) 1447; W.-Y. P. HWANG and H. PRIMAKOFF, Phys. Rev. *16C* (1977) 397.
[21] N. C. MUKHOPADHYAY and J. MARTORELL, Nucl. Phys. *A296* (1978) 461.
[22] P. LEBRUN et al., Phys. Rev. Lett. *40* (1978) 302.
[23] Y. MASUDA et al., Phys. Rev. Lett. *43* (1979) 1083.
[24] Y. NAMBU, Phys. Rev. Lett. *4* (1960) 380; M. GELL-MANN and M. LEVY, Nuovo Cimento *16* (1960) 750.
[25] H. PRIMAKOFF, Nucl. Phys. *A317* (1980) 279.
[26] M. BARDIN et al., Phys. Rev. Lett. *7* (1961) 23.
[27] A. I. ALIKHANOV et al., JETP *11* (1960) 1380; G. Backenstoss et al., Phys. Rev. Lett. *6* (1961) 415.
[28] T. YAMAZAKI, *High Energy Physics and Nuclear Structure* (1979), Vancouver, North Holland, p. 537.
[29] Y. G. BUDYASHOV et al., JETP *31* (1970) 651.